TIJMET, Vol. 002 (2019) 39-45

The International Journal of

Materials and Engineering Technology

ISSN: 2667-4033
TIJMET ID: 190201006 (7 pages)
Type of the Paper: Article
Received 09.02.2019 Revised: 07.08.2019 Accepted: 27.09.2019 Published (Online): 01.10.2019
Journal homepage: http://dergipark.gov.tr/tijmet

TEMPERATURE DISTRIBUTION IN CENTRIFUGAL CASTING WITH PARTIAL SOLIDIFICATION DURING POURING

I. D. ERHUNMWUN[1] and C.E. ETIN-OSA[2]

[1]Department of Production Engineering, University of Benin, P.M.B. 1154, Benin City, Nigeria.
[2]Department of Production Engineering, University of Benin, P.M.B. 1154, Benin City, Nigeria
Email: [1]iredia.erhunmwun@uniben.edu and [2]etinosa.eruogun@uniben.edu

Abstract

In this paper, we have provided the mathematical modeling of the conductive heat transfer in horizontal centrifugal casting which was then used to analyze the temperature distribution in centrifugal casting. The Finite Element Method (FEM) as a numerical tool was used to discretize and analyze the temperature distribution. The result obtained shows the temperature distribution both in the liquid cast region and the mould region. The pouring temperature of the liquid cast into the prepared mould was 1500^{0}C and also to prevent thermal shock, the mould was preheated to a temperature of 250^{0}C. After about 50 secs when the liquid cast has been poured into the mould, the result obtained shows a decrease in temperature from 1407.3477 ^{0}C at a distance of 4.5cm to 1323.0772^{0}C at a distance of 6.5cm from the center of the mould which is the interface between the liquid cast and the mould. Also in the mould region, after about 50 secs, the temperature drops from 755.8252^{0}C at 6.5cm to 350.6205^{0}C at 15.5cm from the center of the mould. The maximum percentage error was 0.81996% and the minimum percentage error was 0.0000%. This comparison was made for the temperature distribution in the cast region and the mold region after about 50 secs when the molten metal has been poured into the mold cavity. This shows that the result obtained from this research is in agreement with the result obtained from Exact Differential Equation Method (EDEM).

Keyword: Centrifugal Casting, Finite Element Method, Heat Transfer, Discretization, Partial Solidification.

1. Introduction

The centrifugal casting processing (vertical or horizontal) is the method of choice for producing HSS shells with improved mechanical performance. However, the centrifugal casting process is complex and difficult to control [1–4] and therefore, numerical modeling is an important tool for understanding and improving the centrifugal casting of 25% Cr-20% Ni steel rolls. Horizontal centrifugal casting is an important industrial process used especially for the production of high-quality seamless tubes and outer shells of work rolls. In this process, the effect of centrifuging is twofold. First, it is the fictitious centrifugal force making the production of axisymmetric hollow castings even possible by pushing the molten metal against the inner wall of the cylindrical mould. Second, the interaction between inertial forces and the vector of the gravitational acceleration induces the so-called pumping effect, responsible for thorough mixing, [5] the growth of fine equiaxed grains, and superior mechanical properties of the cast [6-7].

The technological difficulties involved in casting processes vary considerably according to the metal's melting temperature characteristics, which in turn are related to the physicochemical properties and structures of metals and alloys. These difficulties also involve a series of properties, which include differences in chemical activities between the elements that constitute the alloy, solubility of the gases, method of solidification among the chemical elements, type of molding, and coefficients of solidification shrinkage. On the other hand, the cooling process also affects the flow of cast metal, influencing the mold filling and stability, allowing the occurrence of cooling stresses and properties changes in the final product, and producing variations in the geometrical dimensions, the shape of the surface finish and the quality of the cast part. Some of the properties and characteristics most directly associated with the casting process are as follows, given by [8].
Kamlesh in 2001, carried out a study using the FDM to determine the temperature distribution in horizontal centrifugal casting [9]. Also, Anjo in 2012 studied numerically the steady conduction heat transfer during the solidification of aluminum in green sand mould using FDM in 2D [10]. The numerical simulation of the process of centrifugal casting is challenging, the description of its numerical simulation is not replete. Some papers describe the less complex vertical centrifugal casting process [11]. Therefore, this research paper sort to look into the temperature distribution in horizontal centrifugal casting under the condition that the liquid cast partially solidifies the moment it's been poured into the mould (which has not been studied by any researcher to the best of my understanding). This research also covers both the temperature distribution in the liquid cast region and the mould region.

2. Mathematical formulation

The mathematical models used in centrifugal casting are based especially on heat transfer and solidification consideration of centrifugal casting. A schematic representation of the model of the centrifugal casting is shown in Figure 1. The heat is withdrawn from the liquid region of the casting to the metallic mould, and finally from mould to surrounding. Heat is also radiated away from the inner surface of the casting. As the solidification proceeds by conductive heat transfer through the molten metal in contact with metallic mould, the solid-liquid interface moves away from the metallic mould. The transient radially symmetric heat flow in the cylinder is governed by:

$$\frac{1}{r}\frac{\partial}{\partial r}\left(k_{\xi} r \frac{\partial T_{\xi}}{\partial r}\right) = C_{\xi}\rho_{\xi}\frac{\partial T_{\xi}}{\partial t} \qquad 1$$

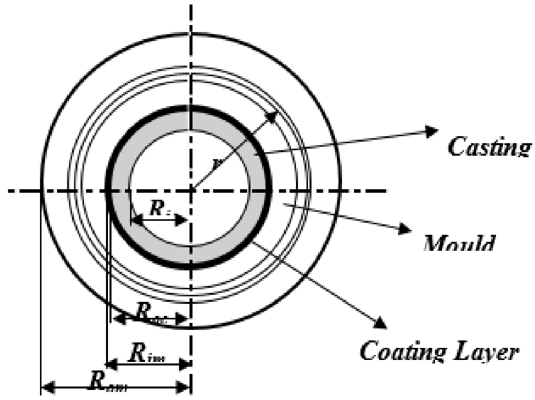

Figure 1. Geometry of horizontal-axis centrifugal casting

Before pouring the melt into the mould, the mould is preheated to a certain temperature to avoid thermal damage to the mould. Therefore, the initial temperature distributions in the casting, mould and shell regions are taken as:

$$T_c = T_p \qquad 2$$

$$T_g = T_m = T_M \qquad 3$$

As soon as the melt comes in contact with the mould wall, temperature of the metal-mould interface increases suddenly. Initial interface temperature is approximated by considering thermal energy conservation within the very thin layer of the metal and the mould in an adiabatic system. Since the heat flow rate from the metal to mould at the beginning is very rapid indeed, it can be stated that the liquid metal within this layer solidifies instantaneously.
In order to find the metal-coating layer interface temperature at time *t=0*, the mould is assumed to be at a temperature T_M and the initial temperature of casting is assumed to be the temperature of the metal as it enters the mould cavity. To find a reasonable approximation to the initial interface temperature, consider an adiabatic system shown in Figure 2.
If the liquidus and solidus lines of a binary system are approximated by straight lines, the fraction of liquid solidified as a function of temperature can be expressed as

$$FS = \frac{T_L - T}{T_L - T_f} \qquad 4$$

where T_L and T_f are the liquidus and solidification front temperatures, respectively.

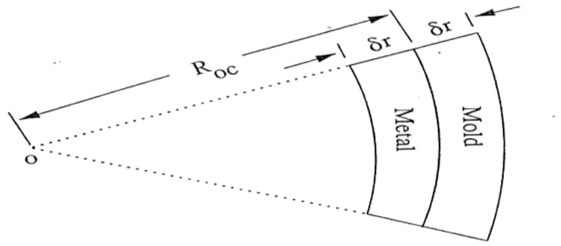

Figure 2: Control volume considered when calculating the initial temperature of metal-mould interface [12]

Equating thermal energy in the system initially to that in the system at equilibrium yields and rearranging terms, T_0 can be written as

$$T_0 = \frac{\rho_L C_L T_P + \rho_g C_g T_M + \dfrac{\rho_L \Delta H T_L}{T_L - T_f}}{\rho_L C_L + \rho_g C_g + \dfrac{\rho_L \Delta H}{T_L - T_f}} \quad 5$$

It is necessary to assume the final state of the metal (liquid, mushy, or solid) in order to determine the initial interface temperature. After estimating $\mathbf{T_0}$ using the appropriate equation according to the assumed condition, its value is checked to ensure that the calculated $\mathbf{T_0}$ falls within the temperature range initially assumed [12].

The boundary conditions in different regions of the casting and mould are as follows:

1. At the inner surface of the casting, i.e., at $r = R_{ic}$,

$$k_{lc} \frac{\partial T_{lc}}{\partial r} = h_2 \left(T_{ci} - T_\beta \right) \quad 6$$

where $T_\beta = \dfrac{T_p + T_a}{2}$ 7

In developing the weak form, we assumed a linear mesh and placed it over the domain. This was done by multiplying Eq. 1 by the weighted function (w) and integrating the final Equation over the domain. This results in the mathematical expression in Eq. 8.

$$\frac{k_\xi}{C_\xi \rho_\xi} \int_{r_A}^{r_B} r \frac{\partial w}{\partial r} \frac{\partial T_\xi}{\partial r} dr + \int_{r_A}^{r_B} w \frac{\partial T_\xi}{\partial t} r dr - wQ_A - wQ_B = 0 \quad 8$$

where $-Q_A = \dfrac{w k_\xi r}{C_\xi \rho_\xi} \dfrac{\partial T_\xi}{\partial r} \Big|_{r_A}$ and $Q_B = \dfrac{w k_\xi r}{C_\xi \rho_\xi} \dfrac{\partial T_\xi}{\partial r} \Big|_{r_B}$ 9

Eq. 8 is referred to as the weak form of the governing.

In the weak form, since the primary variable is simply the function itself, the Lagrange family of interpolation functions is admissible, therefore:

$$T_\xi(r,t) = \sum_{j=1}^{n} \left(T_\xi\right)_j (t) \psi_j^e(r) \quad and \quad w = \psi_i^e(r) \quad 10$$

Substituting eq. 10 into eq. 8, we have:

$$\left[K_{ij}^e\right]\left\{T_\xi\right\}_j + \left[M_{ij}^e\right]\left\{\dot{T}_\xi\right\}_j = \left\{Q_i^e\right\} \quad 11$$

$$\text{where } K_{ij}^e = \frac{k_\xi}{C_\xi \rho_\xi} \int_{r_A}^{r_B} r \frac{\partial \psi_i^e}{\partial r} \frac{\partial \psi_j^e}{\partial r} dr \quad 12$$

$$M_{ij}^e = \int_{r_A}^{r_B} r \psi_i^e \psi_j^e dr \quad 13$$

Next, we use the already developed finite element model of one-dimensional time-dependent problem to describe time approximation schemes and also convert the ordinary differential equation in time to algebraic equation. The most commonly used method for solving eq. 11 is the α family of interpolation in which a weighted average of the time derivative of the dependent variable is approximated to two consecutive time steps by linear interpolation of the values of the variables of the two steps. Therefore, we have:

$$\left[\left[M_{ij}^e\right] + \Delta t_{s+1}\alpha\left[K_{ij}^e\right]\right]\left\{T_\xi\right\}_{j_{s+1}} = \left[\left[M_{ij}^e\right] - \Delta t_{s+1}(1-\alpha)\left[K_{ij}^e\right]\right]\left\{T_\xi\right\}_{j_s} + \Delta t_{s+1}(1-\alpha)\left\{Q_i^e\right\}_s + \Delta t_{s+1}\alpha\left\{Q_i^e\right\}_{s+1} \quad 14$$

Using the Backward Difference Scheme, where $\alpha = 1$, eq. 14 is reduced to eq. 15

$$\left\{T_\xi\right\}_{j_{s+1}} = \left[\left[M_{ij}^e\right] + \Delta t_{s+1}\left[K_{ij}^e\right]\right]^{-1}\left[\left[M_{ij}^e\right]\left\{T_\xi\right\}_{j_s} + \Delta t_{s+1}\left\{Q_i^e\right\}_{s+1}\right] \quad 15$$

2.1. Evaluating the elemental matrices

The one-dimensional Lagrange quadratic interpolation function for the equation becomes:

$$\psi_1(r) = \frac{1}{h_e^2}\left(h_e + r_A - r\right)\left(h_e - 2r + 2r_A\right) \quad 16$$

$$\psi_2(r) = \frac{4}{h_e^2}\left(r - r_A\right)\left(h_e + r_A - r\right) \quad 17$$

$$\psi_3(r) = \frac{-1}{h_e^2}\left(r - r_A\right)\left(h_e - 2r + 2r_A\right) \quad 18$$

The conductivity matrix can be easily derived by substituting the Lagrange interpolation functions in eq. 16 to 18 into eq. 12 respectively, we have:

$$\left[K^e\right]=\frac{k_\xi}{6h_eC_\xi\rho_\xi}\begin{bmatrix} 3h_e+14r_A & -(4h_e+16r_A) & h_e+2r_A \\ -(4h_e+16r_A) & 16h_e+32r_A & -(12h_e+16r_A) \\ h_e+2r_A & -(12h_e+16r_A) & 11h_e+14r_A \end{bmatrix} \quad 19$$

Also, the Enthalpy matrices can be easily derived by substituting the Lagrange interpolation functions in eq. 16 to 18 into eq. 13 accordingly, we have:

$$\left[M^e\right]=\frac{h_e}{60}\begin{bmatrix} h_e+8r_A & 4r_A & -h_e-2r_A \\ 4r_A & 16h_e+32r_A & 4h_e+4r_A \\ -h_e-2r_A & 4h_e+4r_A & 7h_e+8r_A \end{bmatrix} \quad 20$$

3. Results and Discussion

The model has been implemented by using the following thermo physical properties (for casting and mould material), and design and operating parameters. 25% Cr-20% Ni steel is chosen as molten metal and 0.4% Carbon steel as mould material to validate the developed model with results available in literature. Various design and operating parameters, like geometric constants for the casting and the mould, the heat transfer coefficient at different regions of casting and the mould, and initial temperatures of mould and metal used in the analysis are tabulated in Table 1. The cooling conditions at the inner surface of the casting and at the outer surface of the steel mould are defined in terms of heat transfer coefficients h_1 and h_2 respectively, and the heat transfer due to the air gap at the metal-mould interface is varied by the solidified thickness of casting. The results of simulation are presented in the following sections.

Casting material: 25% Cr-20% Ni steel
Mould material: 0.4% Carbon steel
ε_M = 0.4, the value at approximately 300^{0}C.
Coating layer: Silica flour, diatomaceous earth and binder diluted with water

In this analysis, the initial pouring temperature of the liquid cast at time $t=0$ as shown in Table 2 was taken to be *1500^{0}C*. Also, to prevent the mould from collapsing due to a sudden change in temperature, the mould was preheated to a temperature of *250^{0}C*. This temperature represents the initial Mould Temperature. Before pouring the liquid cast into the mould, the temperature of the air in the mould and outside the mould was taken to be *25^{0}C*. This represents the Ambient Temperature.

Table 1: Thermo physical properties of casting, mould material, and coating layer

Thermo Physical Properties	25%Cr-20%Ni Steel	0.4 Carbon Steel	Coating Layer
$K_d\left(cal/cm\sec^0 C\right)$ at 0^0C	0.025	0.126	2x10^{-2}
ρ(g/cm^3)	7.3	7.8	5.7
C(cal/g^{0}C)	0.118	0.1	0.08
T_s(^{0}C)	1300	-	-
T_L(^{0}C)	1400	-	-
T_f(^{0}C)	1300	-	-
ΔH(cal/g)	60	-	-

Table 2: Design and operating parameters used in analysis

Outer diameter of steel mould, (cm)	31
Outer diameter of casting, (cm)	13
Inner diameter of casting, (cm)	9
Damping coefficient between the mould-metal interface, β	0.83
Heat transfer coefficient at outer surface of steel mould (h_2) and at inner surface of casting (h_1), (cal/cm^{2}sec^{0}C)	0.0002
Initial pouring temperature of liquid metal, T_p(^{0}C)	1500
Initial mould temperature, T_M(^{0}C)	250
Ambient temperature, T_a(^{0}C)	25
Emissivity at outer surface of mould, ε_M	0.4

In this case where the metal partially solidifies, it is observed that the rate of temperature drop in the cast region is less than the rate of temperature drop in the liquid cast region considering the case where none of the liquid solidifies as published by Erhunmwun, et al. [13]. It is also observed that the rate of temperature drop in the mould region is more than the rate of temperature drop in the mould region considering the case where none of the liquid solidifies.

Figure 3 shows a graph of temperature against radial displacement at different time in the liquid cast region for the case when the liquid metal partly solidifies. From Figure 3, it is observed also that there is a decrease in temperature in the liquid metal cast with time.

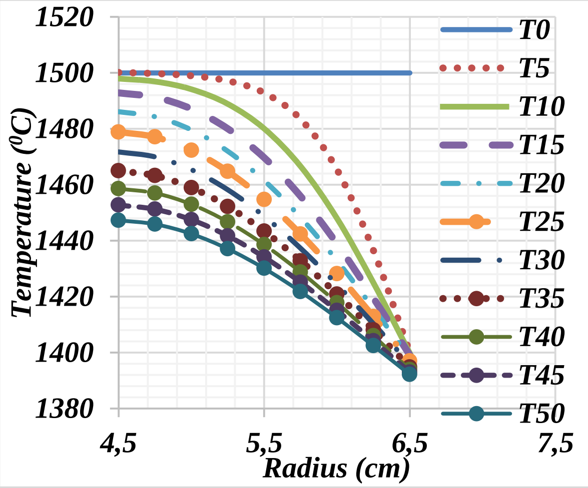

Figure 3. A graph of Temperature against Radius in the liquid cast region

Figure 4 shows a graph of temperature against radial displacement at different time in the mould region for the case when the liquid metal partially solidifies. Again from Figure 4, it can be seen that the mould is preheated to a temperature of *250^{0}C*. This is temperature is uniform all through the region of the mould. As the liquid cast is poured into the mould, it is observed that there is a sudden increase in temperature at the solid metal cast / mould interface from *250^{0}C* to *996.4021^{0}C*. This is due the fact that the heat in the liquid cast is quickly conducted away from the liquid cast into the mould. This increase in temperature was very pronounced in the region close to the solid cast / mould interface. This sudden temperature increase at the interface decreases towards the outer surface of the mould. As time increases, there is a decline in temperature and the heat in the system is finally released in the atmosphere.

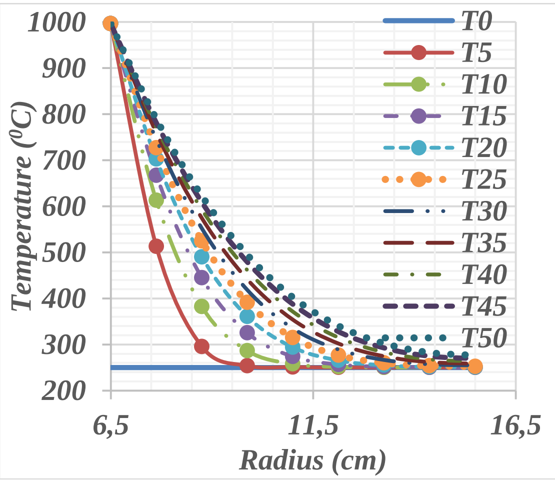

Figure 4. A graph of Temperature against Radius in the mould region

Figure 5 shows a graph of temperature against radial displacement at different time both in the solid matal cast region and the mould region. Between 4.5cm and 6.5cm is the solid and liquid metal cast region and between 6.5cm and 15.5cm is the mould region. Along the 6.5cm line in the radial axis is the interface between the solid metal cast region and the mould region. Along the interface, there is a sudden drop in temperature. At about 10sec after the liquid metal has been poured into the mould, the temperature suddenly droped at the interface from 1399.7524^{0}C to 996.4021^{0}C. Also, at this same time, the temperature at the outer surface of the metal mould has increased to about 250.0563^{0}C.

It observed that from Figure 5 as the liquid metal is poured into the mould, the temperature at the inlet begins to decrease. At about 10sec after pouring the molten metal into the mould, the temperature at the inner surface of the liquid matal cast would have droped to about 1497.9694^{0}C and at about 50sec after pouring, the temperarure would have droped to about 1447.3035^{0}C. Still at 50sec after pouring and at the solid metal cast / mould interface, the temperature droped suddenly from 1392.1460^{0}C at the solid metal cast region to 996.4021^{0}C at the mould region. There after in the mould region, the temperature begins to drop steadily till the outer surface of the mould where the temperature is lost to the atmosphere.

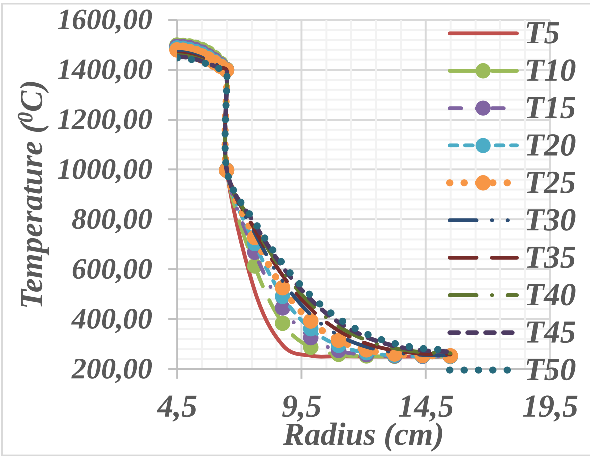

Figure 5. A graph of Temperature against Radius in the liquid cast and mould region

The temperature profiles obtained by this research, for different operating conditions have been shown above in Figure 3 to Figure 5. The trend of temperature profiles obtained in this research using the FEM is similar to those obtained by using the EDEM with some percent of error.

Table 3. Comparison between FEM and EDEM

Radial Distance	FEM	EXACT	% Error
4.5	1407.348	1407.33	-0.0012
4.75	1405.277	1405.262	-0.0011
5	1399.832	1399.817	-0.0011
5.25	1391.383	1391.372	-0.0008
5.5	1380.413	1380.402	-0.0008
5.75	1367.468	1367.462	-0.0004
6	1353.169	1353.164	-0.0004
6.25	1338.153	1338.152	-4.7E-05
6.5	1323.077	1323.077	0.0000
6.5	996.4021	996.4021	0.0000
7.625	790.6284	790.1037	-0.0664
8.75	624.1039	623.5017	-0.0966
9.875	496.0492	495.8438	-0.0414
11	403.2544	403.8336	0.14342
12.125	340.7017	341.9952	0.37822
13.25	302.0875	303.9733	0.62041
14.375	281.7999	283.9851	0.76948
15.5	275.6203	277.8989	0.81996

To validate the result from this research, we compare our result with the result obtained by using the EDEM. Table 3 shows the percentage error between the result from this research and the result obtained by using the EDEM. From the table, the maximum percentage error was 0.81996% and the minimum percentage error was 0.0000%. This comparison was made for the temperature distribution in the cast region and the mold region after about 50 secs when the molten metal has been poured into the mold cavity. This shows that the result obtained from this research is in agreement with the result obtained from using the EDEM.

4. Conclusion

The temperature distribution of cast in horizontal centrifugal casting when the liquid cast partially solidifies as it is poured into the mould has been analysed. Based on the results and discussion presented in the preceding section, the following conclusions can be reached.

The FEM form of the heat conduction model was used in the analysis. Using model, a numerical solution has been developed for horizontal centrifugal casting. The FEM provides the node by node results for temperature distribution. Using FEM, the result obtained was compared with EDEM. It was found that both result gives approximately identical solution for the temperature distribution in centrifugal casting.

References

1. Nastac, L; Valencia, JJ.; Xu, J.; Dong, H. A Computer Model for Simulation of Multi-Scale Phenomena in the Centrifugal Casting of Metal-Matrix-Composites, TMS, Symposium on Materials Processing in the Computer Age III, Nashville, TN, **2000.**
2. Hao, H; Huang, X.; Nastac, L.; Sundarraj, S.; Simkovich, A. Modeling of Centrifugally-Cast TiC/Bronze Metal Matrix Composites, Proceedings of the *Modelling of Casting, Welding and Advanced Solidification Processes VIII*, The Minerals, Metals & Materials Society **1998**, 1015-1022.
3. Lewis III, D.; Singh, M.; in In Situ Composites: Science and Technology, Singh, M.; Lewis, D., editors, (The Minerals, Metals and Materials Society, Warrendale, **1994**, 21.
4. Lajoye, L.; Suery, M.: Proceedings of the International Symposium on Advances in Cast Reinforced Metal Composites, edited by Fishman, SG.; Dhingra, AK. ASM International, Materials Park, OH, **1988**, 15.
5. Esaka, H., Kawai, K., Kaneko, H. and Shinozuka K.: In-Situ Observation of Horizontal Centrifugal Casting using a High-Speed Camera. IOP Conference Series: Materials Science and Engineering, **2012**, 33, 012041.
6. Wei, S; Lampmas, S. Centrifugal Casting. In Centrifugal Casting. Ohio, ASM International; **2008**, 15, 667-673.
7. Kapranos, P.; Carney, C.; Pola, A.; Jolly, M. Advanced Casting Methodologies: Investment Casting, Centrifugal Casting, Squeeze Casting, Metal Spinning, and Batch Casting. Comprehensive Materials Processing, **2014**, 5, 39–67.
8. Campbell, J. “Casting”, Butterworth-Heinemann, Oxford, 1991.
9. Kamlesh (2001): Ph.D. Thesis, BVM Engineering College, Gujarat, India, p. 35.
10. Anjo, V. Numerical Simulation of Steady State Conduction Heat Transfer during the Solidification of Aluminum Casting in Green Sand Mould. Leonardo Electronic Journal of Practices and Technologies, **2012**, 20, 15-24.
11. Kaschnitz, Z. Numerical simulation of centrifugal casting of pipes. IOP Conference Series: Materials Science and Engineering, **2012**, 33012031.
12. Raju, PSS.; Mehrotra, SP. Materials Transactions. JIM, **2000**, 41, 1626–1635.

13. Erhunmwun, ID.; Akpobi, JA.; Osunde, TA. Numerical Determination of the Effects of Pouring Temperature and Mold Preheat Temperature on the Solidification Time in Centrifugal Casting, Journal of the Nigerian Association of Mathematical Physics, **2018**, 48, 4, 31-336